New Conceptual Toxicokinetic Model to Assess Synergistic Mixture Effects between the Aromatic Hydrocarbon β-Naphthoflavone and the Azole

Environmental Science & Technology

pubs.acs.org/est

Article

New Conceptual Toxicokinetic Model to Assess Synergistic Mixture Effects between the Aromatic Hydrocarbon β-Naphthoflavone and the Azole Nocodazole on the CYP1A Biomarker in a Fish Cell Line

Shirin Fallahi, Marie Mlnaříková, Charlotte Alvord, Guttorm Alendal, Håvard G. Frøysa, Torbjörn Lundh, and Malin C. Celander*

Cite This: *Environ. Sci. Technol.* 2020, 54, 13748−13758

Read Online

ACCESS | Metrics & More | Article Recommendations | Supporting Information

ABSTRACT: Toxicokinetic interactions with catabolic cytochrome P450 (CYP) enzymes can inhibit chemical elimination pathways and cause synergistic mixture effects. We have created a mathematical bottom-up model for a synergistic mixture effect where we fit a multidimensional function to a given data set using an auxiliary nonadditive approach. The toxicokinetic model is based on the data from a previous study on a fish cell line, where the CYP1A enzyme activity was measured over time after exposure to various combinations of the aromatic hydrocarbon β-naphthoflavone and the azole nocodazole. To describe the toxicokinetic mechanism in this pathway and how that affects the CYP1A biomarker, the model uses ordinary differential equations. Local sensitivity and identifiability analyses revealed that all the 10 parameters estimated in the model were identified uniquely while fitting the model to the data for measuring the CYP1A enzyme activity. The model has a good prediction power and is a promising tool to test the synergistic toxicokinetic interactions between different chemicals.

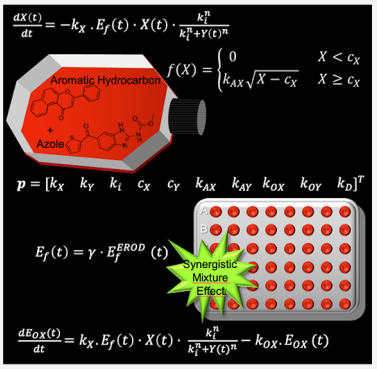

1. INTRODUCTION

Induction of cytochrome P450 1A (CYP1A) in fish can be used as a biomarker to assess exposure to aromatic hydrocarbons in aquatic environments. Induction of CYP1A is typically measured as increased levels of transcription (*i.e.*, CYP1A mRNA/CYP1A protein levels), increased CYP1A enzyme activities, or a combination of both. Aromatic hydrocarbons activate the aryl hydrocarbon receptor (AhR), which results in induction of CYP1A synthesis. The AhR-CYP1A signaling is central in the chemical detoxification pathway in fish.[1] The aquatic environment is also contaminated with other anthropogenic chemicals, including pharmaceuticals.[2,3] Some pharmaceuticals can interfere with the AhR-CYP1A signaling pathway. Hence, fish populations in their natural habitats are exposed to mixtures of chemicals that can interact with the AhR-CYP1A signaling and thereby affect the CYP1A biomarker.[4]

The mixture effect of different chemicals is called an additive effect if there is no direct interaction between the chemicals when they exert their effects. Thus, the chemicals act independently of each other with similar modes of action (MoA) and the mixture effect can be explained by addition. If a mixture gives an effect higher than the additive prediction, this effect is called synergistic.[5] There are established models to assess additive mixture effects such as the concentration addition, the independent action, and the generalized concentration addition models.[6] There are also models that can identify nonadditive mixture effects from response patterns for end points.[7−10] These models are, however, empirical models and lack a mechanistic basis for prediction. For this reason, there is a need for models to assess nonadditive mixture effects in a mechanistic manner, for example, to describe synergistic effects in fish and other vertebrates.

Chemicals with the same or different MoA can interact with each other's detoxification mechanisms and cause adverse toxicokinetic interactions. The value of integrating toxicokinetics, for a better mechanistic understanding to predict interactions between different chemicals in mixtures, has been advocated by the European Commission.[11] A promising approach, using a mechanistic toxicokinetic and toxicodynamic model, was suggested to describe the synergistic mixture effects between azole fungicides and a pyrethroid insecticide in the invertebrate *Daphnia magna*. This model was based on the fact that the synergistic potential of adding azoles could be explained by the azoles occupying the CYP enzymes, which reduces the biotransformation of the insecticide.[12]

Azoles [*e.g.*, clotrimazole, ketoconazole, nocodazole (NOC), omeprazole, prochloraz, and propiconazole] have been shown

Received: July 20, 2020
Revised: September 19, 2020
Accepted: October 1, 2020
Published: October 15, 2020

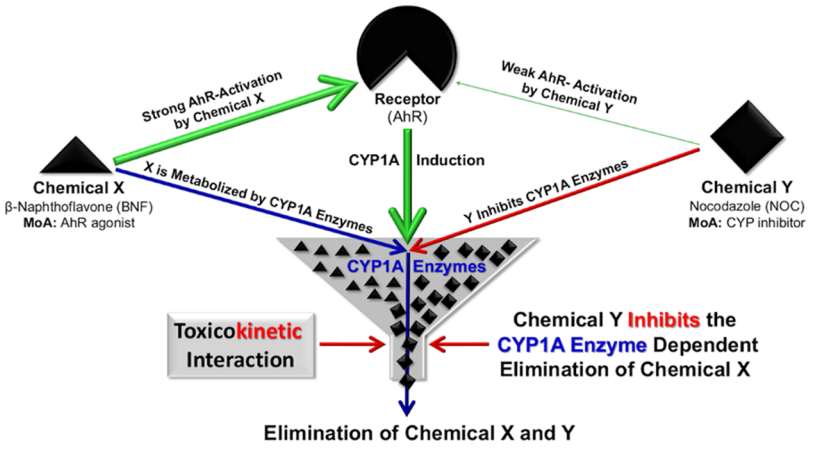

Figure 1. Illustration of the pathway that the model describes. Chemical X (BNF, black triangles) and chemical Y (NOC, black squares) belong to different chemical classes, each with different MoA. Induction of cytochrome P450 1A (CYP1A) is mediated via ligand activation of AhR. Chemical X is a strong ligand to AhR (illustrated by a thick green arrow), which results in strong induction of CYP1A. Chemical Y is a weak ligand to AhR (illustrated by a thin green arrow), which results in low induction of CYP1A. Both X and Y bind to the CYP1A enzymes, where X is metabolized by CYP1A enzymes (blue arrow) and Y inhibits CYP1A enzymes (red arrow). Thus, chemical Y occupies the CYP1A enzymes in the elimination pathway (the gray funnel shape), delaying biotransformation of chemical X, which in turn results in increased biological half-life of chemical X. This toxicokinetic interaction between X and Y results in a synergistic mixture effect. The conceptual model, presented in this study, describes the toxicokinetic interaction between chemicals X and Y in this pathway.

Table 1. Model Parameters and Their Descriptions[a]

	description	unit	value
State Variables			
X	concentrations of unbound BNF molecules	μM	
Y	concentrations of unbound NOC molecules	μM	
E_f	concentrations of free CYP1A enzymes (not used in model equations)	μM	
E_f^{EROD}	EROD activity of free CYP1A enzymes	pmol·(min·mg)$^{-1}$	
E_{OX}	concentrations of CYP1A enzymes occupied by BNF	μM	
E_{OY}	concentrations of CYP1A enzymes occupied by NOC	μM	
t	time	h	
Initial Values			
	initial concentration of BNF	μM	0.1 and 1
	initial concentration of NOC	μM	0, 1, 10, and 25
	initial EROD activity of free CYP1A enzymes	pmol·(min·mg)$^{-1}$	0
	initial concentration of CYP1A enzymes occupied by BNF	μM	0
	initial concentration of CYP1A enzymes occupied by NOC	μM	0
Fixed parameters			
γ	proportionality constant between EROD activity and concentration of free CYP1A	min·mg·L^{-1}	1
n	Hill coefficient		4
Estimated parameters			
k_X	turnover number of the CYP1A enzyme for BNF	(μM·h)$^{-1}$	0.033 ± 0.010
k_Y	turnover number of the CYP1A enzyme for NOC	(μM·h)$^{-1}$	0.039 ± 0.009
k_i	IC_{50} for NOC on EROD activity	μM	1.37 ± 0.049
c_X	minimum concentration of BNF to induce EROD activity	μM	0.063 ± 0.008
c_Y	minimum concentration of NOC to induce EROD activity	μM	0.542 ± 0.061
k_{AX}	rate of number of CYP1A enzymes induced by BNF	h^{-1} (μM)$^{1/2}$	1.339 ± 0.060
k_{AY}	rate of number of CYP1A enzymes induced by NOC	h^{-1}	0.252 ± 0.050
k_{OX}	rate of biotransformation of BNF molecules	h^{-1}	0.375 ± 0.059
k_{OY}	rate of biotransformation of NOC molecules	h^{-1}	0.060 ± 0.012
k_D	rate of CYP1A enzyme degradation	h^{-1}	0.043 ± 0.003

[a]The state variables are defined by eqs 4, 5, and 9−13. The initial values of the state variables are the different doses added to the cell cultures. The model parameters are either fixed or estimated. The estimated parameters are given as the parameter estimate ± standard error. The parameters in the model are fitted to experimental EROD data from a previous study where the cells were exposed to different mixtures of BNF and NOC in a time course study (Table S1).[21,22]

to interact with the CYP system in fish and fish cells.[13−21] Most azoles act as potent inhibitors of CYP1A enzyme activities but weak inducers of CYP1A transcription in fish.[17−19] Previous studies on the *Poeciliopsis lucida* hepatocellular carcinoma (PLHC-1) cell line show that the benzimidazole and microtubule disassembling drug NOC alone acted as

https://dx.doi.org/10.1021/acs.est.0c04839
Environ. Sci. Technol. 2020, 54, 13748−13758

a potent inhibitor of the CYP1A enzyme activity and a weak inducer of CYP1A expression. Compared to β-naphthoflavone (BNF), NOC is 1 order of magnitude less potent and about 50 times less efficient to induce CYP1A expression.[20,21] However, a synergistic mixture effect with NOC and the prototypical AhR agonist, BNF, was seen as increased induction of CYP1A.[21] Although BNF and NOC have different MoA, they seem to share a common elimination pathway. Thus, PLHC-1 cells exposed to NOC were more sensitive to BNF exposures compared to cells exposed to BNF alone.[21] The synergistic mixture effect is based on the hypothesis that NOC occupies the CYP1A enzymes, inhibiting the CYP1A-dependent metabolism of BNF, which in turn enhances the BNF-mediated AhR-CYP1A signaling (Figure 1).

The aim of this study was to create a new conceptual toxicokinetic model to describe the toxicokinetic interaction between BNF and NOC, where the dominant effect of NOC is direct inhibition of CYP1A enzymes and the dominant effect of BNF is induction of CYP1A transcription via activation of AhR. This is a first attempt to create a mathematical bottom-up model for synergistic mixture effects where we fit a multidimensional function to a given experimental data set from a previous study using an auxiliary nonadditive model.[21,22] The time dynamics is a key factor in the toxicokinetic interactions. We hypothesized that by constructing a model using ordinary differential equations (ODEs), we can describe how the concentrations of the chemicals change over time and their resulting effect on the CYP1A biomarker.

2. METHODS

2.1. Development of the Mathematical Model. To describe the mixture effect on the CYP1A biomarker, we construct a model using a set of ODEs. The model also explains the individual effects of each chemical by setting the initial concentrations of the other compounds equal to zero. There are five concentration state variables in the equations, where X represents the unbound BNF, Y represents the unbound NOC, E_f represents the free CYP1A enzymes, E_{OX} represents the CYP1A enzymes occupied by BNF, and E_{OY} represents the CYP1A enzymes occupied by NOC. The state variables, their initial values, and the parameters in the model (*i.e.*, constants) are listed with units in Table 1.

The rate by which the unbound BNF (X) is biotransformed is modeled as

$$\frac{dX(t)}{dt} = -k_X \cdot E_f(t) \cdot X(t) \cdot \frac{k_i^{\,n}}{k_i^{\,n} + Y(t)^n} \quad (1)$$

In this equation, the change in the number of unbound BNF (X) molecules over time is described as a function of the turnover number of the CYP1A enzyme for biotransformation of BNF (k_X) together with the number of molecules for free CYP1A enzymes (E_f), BNF (X), and NOC (Y). The time unit (t) is hours. A Hill function is used to describe that BNF and NOC molecules compete for binding to the free CYP1A enzymes. Consequently, the change in numbers of unbound BNF molecules is affected by the number of NOC molecules over time, which creates a delay in the BNF elimination pathway. The parameters k_i and n in the Hill function describe the competition between the BNF and NOC molecules for the free CYP1A enzymes. The parameter k_i is the concentration of NOC occupying half of the binding sites of the CYP1A enzymes.

The change in the number of unbound NOC (Y) molecules over time is described by second-order kinetics using the turnover number of the CYP1A enzyme for biotransformation of NOC (k_Y), number of molecules for free CYP1A enzymes (E_f), and NOC (Y) giving

$$\frac{dY(t)}{dt} = -k_Y \cdot E_f(t) \cdot Y(t) \quad (2)$$

The change in numbers of free CYP1A enzymes (E_f) over time depends on the number of BNF (X) and NOC (Y) molecules that are occupying the CYP1A enzymes. Hence, binding of BNF and NOC molecules to the CYP1A enzymes results in increased number of occupied CYP1A enzymes (E_{OX} and E_{OY}) and decreased number of free CYP1A enzymes with the degradation rate constant k_D. The rate of change of free CYP1A enzymes is modeled as

$$\frac{dE_f(t)}{dt} = -k_X \cdot E_f(t) \cdot X(t) \cdot \frac{k_i^{\,n}}{k_i^{\,n} + Y(t)^n} - k_Y \cdot E_f(t) \cdot Y(t) + f(X) + g(Y) + k_{OX} \cdot E_{OX}(t) + k_{OY} \cdot E_{OY}(t) - k_D \cdot E_f(t) \quad (3)$$

The parameters k_{OX} and k_{OY} are the biotransformation rate constants of BNF and NOC molecules, whereas the functions $f(X)$ and $g(Y)$ describe the activation of the AhR-CYP1A signaling by BNF and NOC, respectively.

The activation of AhR is controlled by the number of BNF (X) and NOC (Y) molecules in the cells, in particular, the number of BNF molecules. This is because BNF is more than 50 times more effective and around 10 times more potent compared to NOC in activating the AhR-CYP1A signaling.[20,22] The functions $f(X)$ and $g(Y)$ are therefore included to describe this dependency for the activation of AhR, as described in eqs 4 and 5

$$f(X) = \begin{cases} 0 & X < c_X \\ k_{AX}\sqrt{X - c_X} & X \geq c_X \end{cases} \quad (4)$$

$$g(Y) = \begin{cases} 0 & Y < c_Y \\ k_{AY}(Y - c_Y) & Y \geq c_Y \end{cases} \quad (5)$$

The values of c_X and c_Y are the respective threshold concentrations of BNF and NOC required to activate AhR-CYP1A. Equivalently, the parameters k_{AX} and k_{AY} describe the rates of BNF-induced and NOC-induced CYP1A enzymes, respectively.

The rate of change for occupied CYP1A enzymes by BNF (E_{OX}) and NOC (E_{OY}) are modeled as

$$\frac{dE_{OX}(t)}{dt} = k_X \cdot E_f(t) \cdot X(t) \cdot \frac{k_i^{\,n}}{k_i^{\,n} + Y(t)^n} - k_{OX} \cdot E_{OX}(t) \quad (6)$$

$$\frac{dE_{OY}(t)}{dt} = k_Y \cdot E_f(t) \cdot Y(t) - k_{OY} \cdot E_{OY}(t) \quad (7)$$

The BNF and NOC molecules that occupy CYP1A enzymes are being biotransformed by the CYP1A enzymes. Next, their metabolites are released from the CYP1A enzymes and the previously occupied CYP1A enzymes (E_{OX} and E_{OY}) become free. The biotransformation rate constants are k_{OX} and k_{OY}. The number of free CYP1A enzymes (E_f) consequently increases and are available for the next cycle of biotransforma-

https://dx.doi.org/10.1021/acs.est.0c04839
Environ. Sci. Technol. 2020, 54, 13748−13758

tion. The CYP1A biotransformation reduces the numbers of BNF and NOC molecules, and when there are too few molecules to activate AhR, no more free CYP1A enzymes are being synthesized. The remaining CYP1A will be degraded and the numbers of E_f will decrease.

The measured data for the free CYP1A enzymes is the diagnostic ethoxyresorufin-*O*-deethylase (EROD) activity that is assumed to be proportional to the concentration of free CYP1A enzymes. This assumption is justified by the fact that only free CYP1A enzymes can carry out the EROD activity. For this reason, we express the concentration of the free CYP1A enzymes as

$$E_f(t) = \gamma \cdot E_f^{EROD}(t) \tag{8}$$

The parameter γ is a proportionality constant and $E_f^{EROD}(t)$ is the EROD activity of the free enzymes that can be measured. The model equations then become

$$\frac{dX(t)}{dt} = -k_X \cdot \gamma \cdot E_f^{EROD}(t) \cdot X(t) \cdot \frac{{k_i}^n}{{k_i}^n + Y(t)^n} \tag{9}$$

$$\frac{dY(t)}{dt} = -k_Y \cdot \gamma \cdot E_f^{EROD}(t) \cdot Y(t) \tag{10}$$

$$\begin{aligned}\frac{dE_f^{EROD}(t)}{dt} &= -k_X \cdot E_f^{EROD}(t) \cdot X(t) \cdot \frac{{k_i}^n}{{k_i}^n + Y(t)^n} \\ &- k_Y \cdot E_f^{EROD}(t) \cdot Y(t) + \frac{f(X)}{\gamma} + \frac{g(Y)}{\gamma} + \frac{k_{OX}}{\gamma} \cdot E_{OX}(t) \\ &+ \frac{k_{OY}}{\gamma} \cdot E_{OY}(t) - k_D \cdot E_f^{EROD}(t)\end{aligned} \tag{11}$$

$$\begin{aligned}\frac{dE_{OX}(t)}{dt} &= k_X \cdot \gamma \cdot E_f^{EROD}(t) \cdot X(t) \cdot \frac{{k_i}^n}{{k_i}^n + Y(t)^n} \\ &- k_{OX} \cdot E_{OX}(t)\end{aligned} \tag{12}$$

$$\frac{dE_{OY}(t)}{dt} = k_Y \cdot \gamma \cdot E_f^{EROD}(t) \cdot Y(t) - k_{OY} \cdot E_{OY}(t) \tag{13}$$

Hence, we model the EROD activity that can be compared with the data.[21,22] Equation 11 is the rate of change in the EROD activity of free CYP1A enzymes (E_f^{EROD}) over time. Note that the two functions $f(X)$ and $g(Y)$ have not been changed and are given by eqs 4 and 5.

2.2. Experimental Data Used. The PLHC-1 is an established cell line used in aquatic toxicology and suggested as an useful tool for mechanistic studies of regulation and function of CYP1A.[23,24] So far, only one CYP1A immunoreactive protein has been detected in PLHC-1 cells treated with BNF.[25] In addition, a partial CYP1A cDNA sequence was isolated from BNF-treated PLHC-1 cells.[20] The data used to estimate the parameters in the model were obtained from a previous study using PLHC-1 cells that had been treated with the carrier vehicle and different doses of BNF (0.1 and 1 μM) and NOC (1, 10, and 25 μM), alone or mixed together, and measured at five different times (6, 12, 24, 48, and 72 h).[21,22] The CYP1A-mediated EROD activities were analyzed in that study.[21,22] Data from four biological replicates (*i.e.*, four separate experiments each of which representing the mean of four technical replicates) were used during the parameter estimation.[22] The raw data used to parameterize and validate the model are given in Table S1. The effects of BNF and NOC differ with BNF 10 times more potent and 50 times more effective compared to NOC for activation of the AhR-CYP1A signaling.[20,22] However, the impact of NOC is still significant because the concentration of NOC added to the cells are up to 250 times higher than for BNF and NOC is a potent inhibitor of the CYP1A activity.[21,22]

2.3. Parameter Estimation. The model was implemented using the R software.[26] The model has two parameters (n and γ) that were fixed before the estimation procedure. The parameter n is the Hill coefficient and represents the inhibition of the BNF biotransformation by the NOC molecules. We proposed a set {2, 3, 4, 6, 10} of possible values for n and performed the estimation procedure for each of them. Based on this, the value of n was set to 4 because that made the remaining parameters best able to fit the data. The proportionality constant γ in eq 8 was set to 1 min·mg·L^{-1}. The remaining 10 parameters to be estimated are denoted by the vector

$$\boldsymbol{p} = [k_X \;\; k_Y \;\; k_i \;\; c_X \;\; c_Y \;\; k_{AX} \;\; k_{AY} \;\; k_{OX} \;\; k_{OY} \;\; k_D]^T$$

The initial values for the concentrations of BNF (X) and NOC (Y) were set to the concentrations that the cells have been dosed with at $t = 0$. For each of the six treatments used to develop the model, the initial values of the state variables were therefore set to

Treatment 1 **Treatment 2** **Treatment 3** **Treatment 4**

$$\begin{bmatrix} X^0 \\ Y^0 \\ E_f^{EROD\,0} \\ E_{OX}{}^0 \\ E_{OY}{}^0 \end{bmatrix} = \begin{bmatrix} 0.1 \\ 0 \\ 0 \\ 0 \\ 0 \end{bmatrix} \quad \begin{bmatrix} X^0 \\ Y^0 \\ E_f^{EROD\,0} \\ E_{OX}{}^0 \\ E_{OY}{}^0 \end{bmatrix} = \begin{bmatrix} 0.1 \\ 1 \\ 0 \\ 0 \\ 0 \end{bmatrix} \quad \begin{bmatrix} X^0 \\ Y^0 \\ E_f^{EROD\,0} \\ E_{OX}{}^0 \\ E_{OY}{}^0 \end{bmatrix} = \begin{bmatrix} 0.1 \\ 10 \\ 0 \\ 0 \\ 0 \end{bmatrix} \quad \begin{bmatrix} X^0 \\ Y^0 \\ E_f^{EROD\,0} \\ E_{OX}{}^0 \\ E_{OY}{}^0 \end{bmatrix} = \begin{bmatrix} 0.1 \\ 25 \\ 0 \\ 0 \\ 0 \end{bmatrix}$$

Treatment 5 **Treatment 6**

$$\begin{bmatrix} X^0 \\ Y^0 \\ E_f^{EROD\,0} \\ E_{OX}{}^0 \\ E_{OY}{}^0 \end{bmatrix} = \begin{bmatrix} 1 \\ 1 \\ 0 \\ 0 \\ 0 \end{bmatrix} \quad \begin{bmatrix} X^0 \\ Y^0 \\ E_f^{EROD\,0} \\ E_{OX}{}^0 \\ E_{OY}{}^0 \end{bmatrix} = \begin{bmatrix} 1 \\ 25 \\ 0 \\ 0 \\ 0 \end{bmatrix}. \tag{14}$$

To estimate the parameters in the model, the EROD data at the five time points for the one single treatment and the five different mixture treatments have been used. To compare the simulated EROD activity of free CYP1A enzymes from the model against its observations, we define a cost function, cost($\mathbf{p}$), as[27]

$$\text{cost}(\boldsymbol{p}) = \sum_{i=1}^{6} \sum_{j=1}^{5} \sum_{k=1}^{4} [\log((E_{f,\text{model}}^{EROD})_j^i + 1) - \log((E_{f,\text{experiment}}^{EROD})_j^{i,k} + 1)]^2 \tag{15}$$

Equation 15 is the sum of squares of the logarithmic residuals of the EROD activity of free CYP1A enzymes from the model ($E_{f,\text{model}}^{EROD}$) versus its experimental value ($E_{f,\text{experiment}}^{EROD}$), represented by EROD data. It should be noted that in the cost function, one is added to the values of $E_{f,\text{model}}^{EROD}$ and $E_{f,\text{experiment}}^{EROD}$ to avoid numerical instability. We summed over six treatments with four biological replicates at five time points. The estimated values for the parameters in $\boldsymbol{p}$ are those that minimize cost($\boldsymbol{p}$). The modFit function from the flexible modeling environment (FME) package in R[28] was used to perform the box constraint optimization. This method is appropriate to use because of non-negativity constraints on the parameters. The parameters in the model (*i.e.*, constants) and their fixed or fitted values are listed in Table 1.

https://dx.doi.org/10.1021/acs.est.0c04839
Environ. Sci. Technol. 2020, 54, 13748−13758

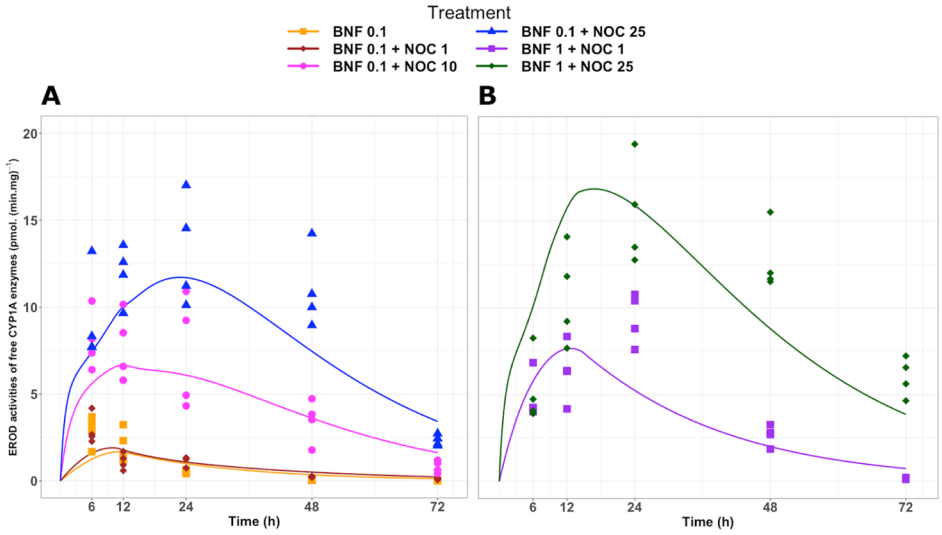

Figure 2. Fitted values for EROD activity of free CYP1A enzymes. The solid lines depict the EROD activity of free CYP1A enzymes from the model fitted to the experimental EROD data [pmol·(min·mg protein)$^{-1}$] (Table S1). The model is described by eqs 4, 5 and 9−13 and the parameters are listed in Table 1. The circles, triangles, squares, and rhombuses represent EROD data from six independent experiments where the cells are exposed to: (A) Treatment (1) 0.1 μM BNF (orange squares), Treatment (2) 0.1 μM BNF + 1 μM NOC (brown rhombuses), Treatment (3) 0.1 μM BNF + 10 μM NOC (pink circles), and Treatment (4) 0.1 μM BNF + 25 μM NOC (blue triangles) and (B) Treatment (5) 1 μM BNF + 1 μM NOC (purple squares) and Treatment (6) 1 μM BNF + 25 μM NOC (green rhombuses). In all treatments, the EROD activities have been measured at five different time points from 6 to 72 h.[21,22] All experimental data are provided in Table S1.

2.4. Global Sensitivity Analysis. Global sensitivity analysis (GSA) is a tool to describe how the uncertainty in the model parameters can influence the uncertainty in the model output.[29] GSA was performed to provide an overview of the sensitivity of the EROD activity of free CYP1A enzymes to uncertainty in the parameter values. GSA identifies the most influential parameters on the model output and identifies parameters that the model output is insensitive to.

The global sensitivity of the EROD activity of free CYP1A enzymes to changes in each parameter (Table 1) was analyzed using experimental EROD data.[21,22] The GSA was performed using the senseRange function from the FME package in R.[28] For each of the parameters, a random sample of 1000 values was drawn using a log-uniform distribution on the interval from the estimated value divided by 10 to the estimated value multiplied by 10. By using this distribution, the expected number of values in the sample below and above the estimated value will be equal.

Next, the global sensitivity of the EROD activity of free CYP1A enzymes was estimated by varying one parameter at the time using the sample described above and fixing the remained parameters at their nominal values. The five coupled ODEs in eqs 9−13 were solved numerically using the *ode* function from the deSolve package in R.[30] This was carried out to calculate the EROD activity of free CYP1A enzymes over time for each parameter set and for each of the six different treatments represented in eq 14.

2.5. Local Sensitivity Analysis. A parameter is practically nonidentifiable if it is not possible to determine a unique value for it through fitting the model to the data. The two main sources of practical nonidentifiability were analyzed: (1) lack of influence of a parameter on the EROD activity of free CYP1A enzymes (E_f^{EROD}) as the measurable model output and (2) interdependence among the parameters.[31]

The local sensitivity analysis (LSA) was performed to assess the sensitivity of the EROD activity of free CYP1A enzymes (E_f^{EROD}), as the measurable model output, with respect to small changes in the estimated parameters (Table 1). The sensitivity of the EROD activity of free enzymes to change in the parameter p_l, while all other parameters were fixed at their nominal values, was computed at the five time points for each treatment experiment through

$$s_l = \frac{\partial E_f^{EROD}}{\partial p_l}, \qquad l = 1, ..., 10 \tag{16}$$

The sensitivity values were estimated numerically using the sensFun function from the FME package in R.[28] The parameter value p_l was perturbed by 1%. In order to take into account the changes in time and across experiments, the root-mean-squared sensitivity was computed for each parameter p_l

$$s_l^{msqr} = \sqrt{\frac{1}{n}\sum_{q=1}^{n}(s_l)_q^2}, \qquad l = 1, ..., 10 \tag{17}$$

This was summed over all five time points for each EROD data in the six different treatment experiments, that is, $n = 30$. The collinearities for all combinations of the 10 parameters in $\boldsymbol{p}$ were tested using the Collin function from the FME package in R.[28]

3. RESULTS AND DISCUSSION

The aim of the present study was to provide a new mathematical bottom-up model to describe the synergistic mixture effect between two different classes of chemicals on a mechanistic level. Experimental data on CYP1A biomarker responses in PLHC-1 exposed to BNF and NOC alone or in binary mixtures were used. The model successfully predicts the changes in CYP1A-mediated EROD activities of free CYP1A enzymes over time by fitting the model to experimental EROD data. In addition, 10 parameters could be estimated in the model.

https://dx.doi.org/10.1021/acs.est.0c04839
Environ. Sci. Technol. 2020, 54, 13748−13758

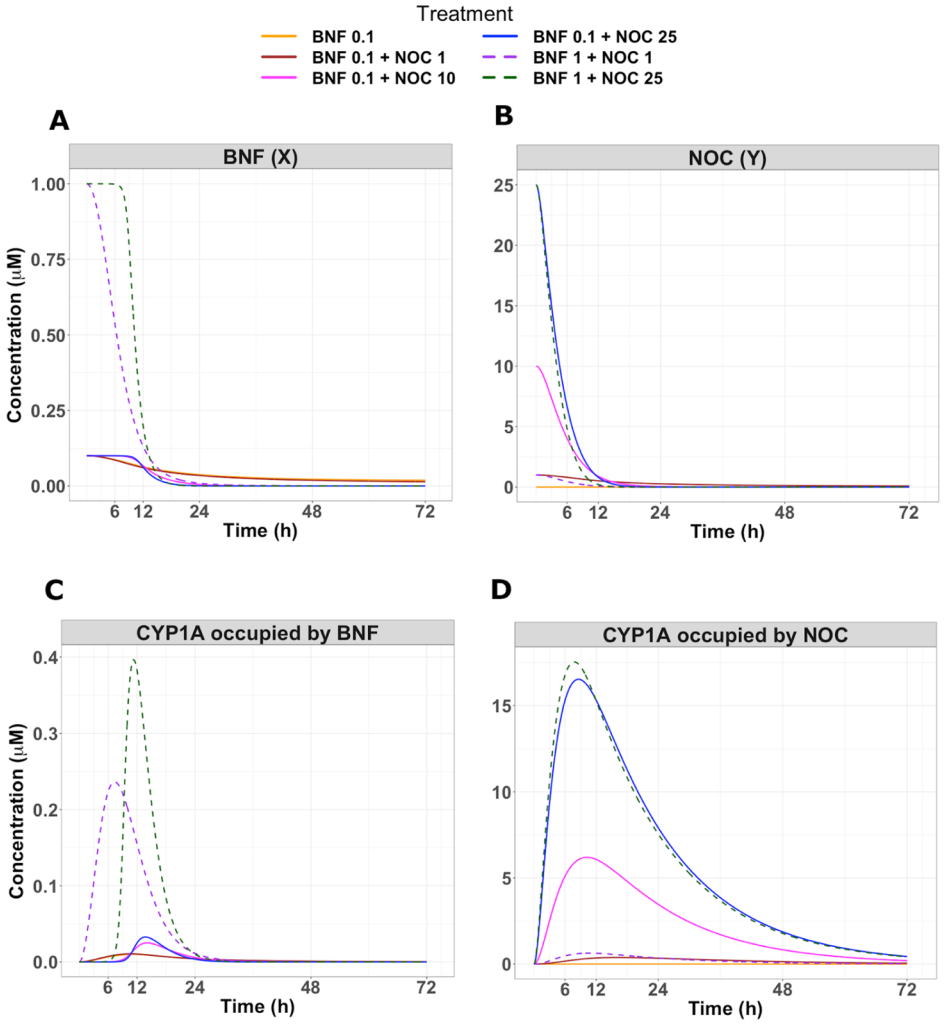

Figure 3. Model predictions for four state variables. (A) Model predictions of BNF (X) concentrations, (B) model predictions of NOC (Y) concentrations, (C) model predictions of number of CYP1A enzymes occupied by BNF (E_{OX}), (D) model predictions of number of CYP1A enzymes occupied by BNF (E_{OY}). The plots depict the model predictions based on the parameters derived from the fit to experimental EROD data (Table S1) from six different treatment experiments: Treatment (1) 0.1 μM BNF (orange solid line), Treatment (2) 0.1 μM BNF + 1 μM NOC (brown solid line), Treatment (3) 0.1 μM BNF + 10 μM NOC (pink solid line), Treatment (4) 0.1 μM BNF + 25 μM NOC (blue solid line), Treatment (5) 1 μM BNF + 1 μM NOC (purple dashed line), and Treatment (6) 1 μM BNF + 25 μM NOC (green dashed line). The model is described by eqs 4, 5 and 9−13 and the parameters are listed in Table 1. In all treatments, the EROD activities have been measured at five different time points from 6 to 72 h.[21,22]

3.1. Model Predictions. The parameters in the model were first estimated using the EROD data from six different treatment experiments.[21,22] The fitted values for the EROD activity of free CYP1A enzymes from the model are shown in Figure 2. The optimal value of cost function in eq 15 was equal to 13.63. This value corresponds to the mean value of the fraction $(E^{EROD}_{f,model} + 1)/(E^{EROD}_{f,experiment} + 1)$ equals to 1.05, which is good because it is close to a value of 1.00 that corresponds to a perfect fit.

The fitted values for the number of free CYP1A enzymes in cells cotreated with 1, 10, or 25 μM NOC, together with either 0.1 or 1 μM BNF, were in good agreement with the experimental data (Figure 2A,B). In addition, there is a satisfactory agreement between the fits for the number of free CYP1A enzymes over time in cells treated with 0.1 μM BNF alone and the experimental data[21,22] (Figure 2A). Because no significant induction of CYP1A activities could be measured in cells treated with 1, 10, or 25 μM NOC alone (Table S3), compared to that in vehicle control cells, no comparison with fitted values was made for those treatments.

The model predicts the four concentration state variables, X, Y, E_{OX}, and E_{OY}, over time (Figure 3). The model shows that increasing the concentration of NOC (at $t = 0$) from 1 to 10 or 25 μM results in slower BNF biotransformation rates. In fact, the model predicts no BNF biotransformation during the first 5−6 h in cells cotreated with 25 μM of NOC and BNF (Figure 3A). This supports our hypothesis that the presence of 25 μM NOC delays the elimination of BNF molecules, which means that more CYP1A enzymes are occupied by BNF after 6 h compared to cells that have been coexposed with a low concentration (1 μM) of NOC (Figure 3C). The model predicts that most of the CYP1A enzymes are being occupied by NOC molecules in a NOC dose-dependent manner during the first 6 h (Figure 3D). In accordance, the model predicts that almost no CYP1A enzymes are occupied by BNF during the first 6 h in the presence of either 10 or 25 μM NOC. The time delay for BNF to bind to free CYP1A enzymes is about 5

https://dx.doi.org/10.1021/acs.est.0c04839
Environ. Sci. Technol. 2020, 54, 13748−13758

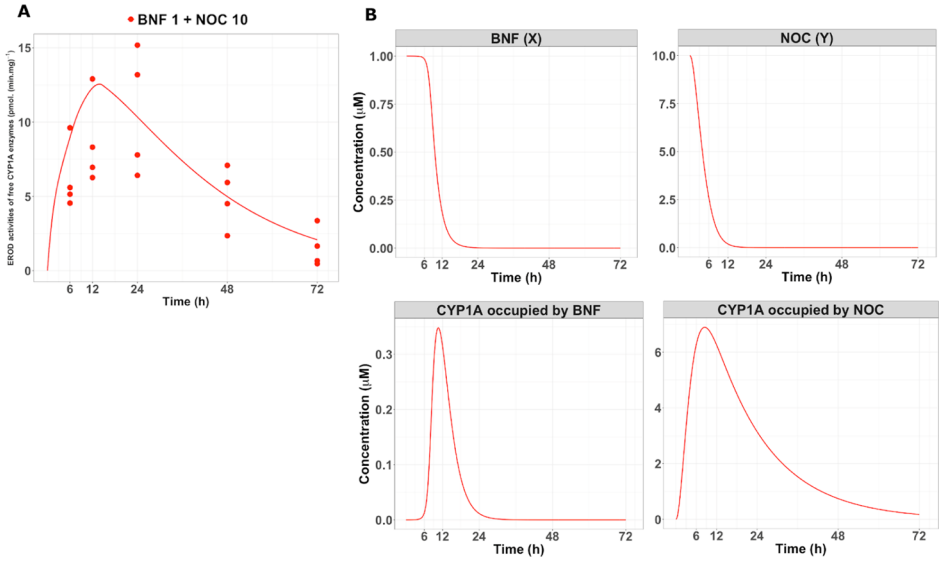

Figure 4. Model validation. (A) The model was validated using data from an additional experiment, Treatment (7) 1 μM BNF + 10 μM NOC (red circles). The model prediction for the EROD activity of free CYP1A enzymes from the model (solid red line) is compared with the experimental EROD data (pmol·(min·mg protein)$^{-1}$) (Table S1).[21,22] (B) Model predictions of changes in the concentrations of BNF (X) and NOC (Y) molecules over time (top panel). Model predictions of the changes in the number of CYP1A enzymes occupied by BNF (E_{OX}) and NOC (E_{OY}) over time (bottom panel). The model is described by eqs 4, 5, and 9−13 and the parameters are listed in Table 1. The experimental data are provided in Table S1.

h shorter for the cells cotreated with 1 μM NOC compared to cells treated with 25 μM NOC (Figure 3A,C). We conclude that it is the delayed elimination of BNF by NOC inhibition of CYP1A enzymes that causes the synergistic mixture effect on the CYP1A-mediated EROD activity.

3.2. Model Validation. The model was validated with data from a seventh experiment,[21,22] Treatment (7) 1 μM BNF + 10 μM NOC shown in Figure 4, which was not used in the parameter estimation procedure.

Treatment 7 used for model validation

$$\begin{bmatrix} X^0 \\ Y^0 \\ E_f^{EROD^0} \\ E_{OX}^0 \\ E_{OY}^0 \end{bmatrix} = \begin{bmatrix} 1 \\ 10 \\ 0 \\ 0 \\ 0 \end{bmatrix}$$

The model prediction for the EROD activity of free CYP1A enzymes is in good agreement with the experimental values of EROD activities from Treatment 7 (Figure 4A). The model predicts how the numbers of CYP1A enzymes occupied by BNF and NOC change over time (Figure 4B, bottom panel). The model also predicts that BNF is not being biotransformed by CYP1A enzymes during the first 5 h in the presence of 10 μM NOC (Figure 4B, top panel).

The validation test shows that the model has good prediction power and can be used to test different combinations of two chemicals and their effect on the EROD activity of free CYP1A enzymes (Figure 4).

3.3. Global Sensitivity Analysis. The ranges from GSA for the EROD activity of free CYP1A enzymes are illustrated using 5−95, 25−75, and 50% (median) quantiles (Figure 5).

The GSA revealed a high sensitivity of the EROD activity of free CYP1A enzymes in all treatments to changes in the CYP1A degradation rate (k_D). To reduce the uncertainty in the model predictions, the value of k_D should therefore be estimated with low uncertainty. In addition, the GSA indicated that changes in the biotransformation rate of BNF (k_{OX}) have no or insignificant individual effect on the robustness of the dynamics of free CYP1A enzymes. To rank the k_{OX} as a noninfluential parameter on the dynamics of free CYP1A enzymes, further analysis is required to calculate the joint effect of this parameter because of its interaction with the other parameters. This can be beneficial for model simplification but was not the main focus of this study. Hence, the GSA revealed that k_D is an influential parameter. It also confirmed that the number of free CYP1A enzymes over time is more sensitive to the changes in the threshold concentration of BNF to induce EROD activity (c_X) compared to the changes in the threshold concentration of NOC to induce EROD activity (c_Y) (Figure 5).

3.4. LSA and Practical Identifiability. The first source of practical nonidentifiability is assessed by computing the sensitivity values of E_f^{EROD} using eq 16. The LSA indicated that the three parameters k_D, k_X, and k_Y have the largest negative average effects on the EROD activity of free CYP1A enzymes and are followed by c_X, c_Y, and k_i, respectively. The other four parameters on an average have positive effects on the EROD activity of free enzymes, with k_{OX} being the parameter with the least effect (Table 2). This is in good agreement with the results from GSA (Figure 5). The sensitivity values of the 10 parameters at each time point for the six treatments are provided in Figure S1.

A parameter with no or insignificant effect on the EROD activity of free CYP1A enzymes was classified as a practically nonidentifiable parameter. It has been suggested that the threshold value classified as a nonidentifiable parameter is 4 orders of magnitude lower than the maximum root-mean-squared value.[31] All of the 10 parameters are above this cutoff value of 0.012 (Table 2). Hence, all the 10 model parameters have significant effects on the EROD activity of free CYP1A

https://dx.doi.org/10.1021/acs.est.0c04839
Environ. Sci. Technol. 2020, 54, 13748−13758

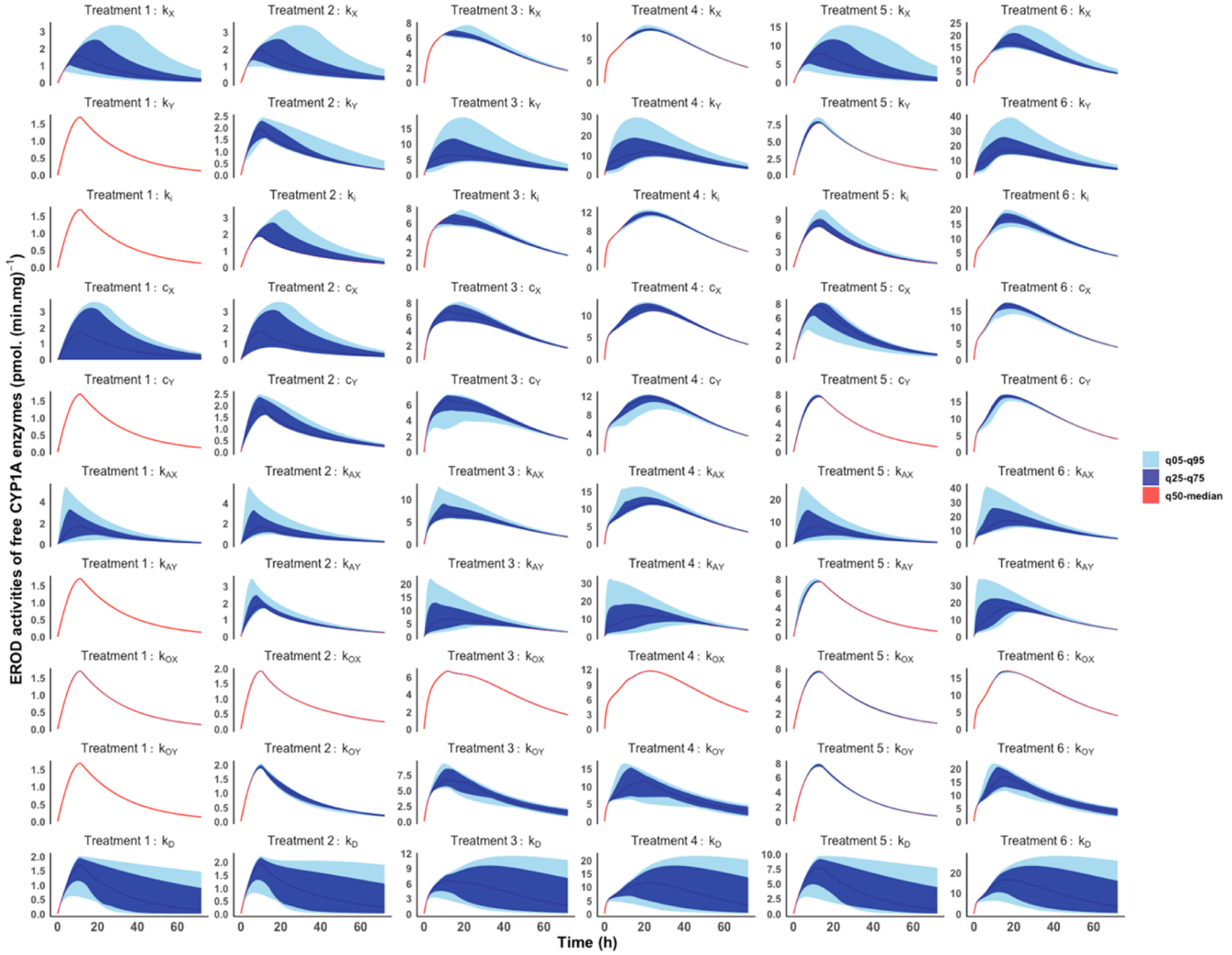

Figure 5. GSA: Sensitivity range of the EROD activities[22] of free CYP1A enzymes over time to changes in one parameter per row is illustrated. The sensitivity ranges are depicted by using 5−95% (light blue), 25−75% (dark blue), and 50% (red) quantiles of the EROD activities of free CYP1A values (vertical axis) estimated by the model on the time interval from dosing (t = 0) to t = 72 h (horizontal axis) for six different treatments: Treatment (1) 0.1 μM BNF, Treatment (2) 0.1 μM BNF + 1 μM NOC, Treatment (3) 0.1 μM BNF + 10 μM NOC, Treatment 4) 0.1 μM BNF + 25 μM NOC, Treatment (5) 1 μM BNF + 1 μM NOC, and Treatment (6) 1 μM BNF + 25 μM NOC.

Table 2. Statistics of LSA of EROD Activity of Free CYP1A Enzymes[a]

parameter	s_l^{msqr}	mean
k_X	31.16	−14.61
k_Y	64.55	−29.28
k_i	0.371	−0.17
c_X	25.55	−12.19
c_Y	1.009	−0.47
k_{AX}	2.185	0.94
k_{AY}	11.99	5.32
k_{OX}	0.072	0.01
k_{OY}	12.34	6.20
k_D	120.2	−54.59

[a] s_l^{msqr} are the root-mean-squared sensitivity measures defined in eq 17, and the mean values are the average of the sensitivity values illustrated in Figure S1.

enzymes with the experimental EROD data. This indicates a strength of the model because the first source of practical nonidentifiability is not a problem.

The parameters may also interfere with each other. Because of the interdependence among the parameters, the possible effect of each parameter on the EROD activity of free CYP1A enzymes may be compensated by change(s) in other parameter(s), known as parameter collinearity. A parameter set with collinearity index above 20 is considered as a nonidentifiable set.[32]

The maximum values of collinearity indices for sets inholding different combinations of the parameters two-ten were 5.60, 8.06, 9.54, 11.58, 14.43, 15.07, 15.58, 16.50, and 17.39, respectively. The collinearity index for all the 10 parameter combinations is provided in Figure S2. The collinearity analysis indicated that all sets with different combinations of parameters had a collinearity index below 20. This led us to conclude that by using the experimental EROD data, unique values for each of the 10 parameters in the model can be estimated simultaneously. Moreover, non-identifiability due to collinearity between parameters is not a problem.

Azoles have been shown to interact with CYP enzymes, including CYP1A in fish.[13−18] For example, ketoconazole was

https://dx.doi.org/10.1021/acs.est.0c04839
Environ. Sci. Technol. 2020, 54, 13748−13758

shown to act as a potent noncompetitive inhibitor of microsomal CYP1A activities in Atlantic cod.[18] Coexposure of ketoconazole that inhibits CYP1A and CYP3A enzymes resulted in increased sensitivity to ethinylestradiol exposure in rainbow trout.[19] Synergistic effects between antifungal azoles and insecticides have earlier been reported. Thus, the azole prochloraz inhibited the biotransformation of a pyrethroid, resulting in increased insecticide toxicity in honeybees coexposed to prochloraz.[33] The azole-mediated inhibition of CYP-dependent detoxification of pesticide was suggested being the main mechanism behind the synergizing effect of azoles on pesticide toxicity.[12] However, the synergistic effect of antifungal azoles on pyrethroid insecticide toxicity was not correlated with the azole inhibition strength on the CYP-mediated ethoxycoumarin-*O*-deethylase activity in two aquatic invertebrates, implying that the mechanisms behind the synergism are more complex.[34] There also seem to be species differences in enzyme susceptibility toward azoles.[35] In PLHC-1 cells, coexposure to the azole NOC delayed the response to BNF exposures, indicating that NOC prevents biotransformation of BNF, presumably by inhibition of CYP1A enzymes.[21] This suggests a delayed CYP1A-mediated biotransformation of BNF in the presence of NOC. Delayed biotransformation for benzo[*a*]pyrene was demonstrated in two rainbow trout cell lines (RTL-W1 and RTgutGC) coexposed with the CYP1A (EROD) inhibitor α- BNF.[36] Hence, inhibition of CYP metabolism can increase the biological half-life of aromatic hydrocarbons, resulting in increased sensitivity to exposures to aromatic hydrocarbons.

The synergistic mixture effect with α-cypermethrin and two azoles in *D. magna* correlated with the inhibition of the CYP-mediated EROD activity by prochloraz and to some extent with the inhibition by propiconazole. It was suggested that a toxicokinetic and toxicodynamic model could be a tool to test the mechanisms of interactions between chemicals.[12] In the present study, we also use a toxicokinetic approach focusing on the inhibition of CYP1A enzyme activity by NOC, by using a Hill function to model the competition between the azole NOC and the AhR agonist BNF. The time that these two chemicals are competing and the steepness of the rate of biotransformation of BNF depend on the Hill coefficient, which was fixed at a preselected value to optimize the model fit to the data. Here, the model might not give a real estimation on how the biotransformation of BNF is controlled by NOC. The model can be further refined in future studies by including chemical data.

The new model presented here successfully predicts the changes in the EROD activities of free CYP1A enzymes over time by fitting the model to experimental EROD data with given mixtures of BNF and NOC. Ten parameters could be estimated in the model. We hypothesize that the synergistic effect is a result of NOC-mediated inhibition of the CYP1A-dependent clearance of BNF. Synergistic mixture effects were seen with two other azoles, clotrimazole and prochloraz, in PLHC-1 cells. These azoles also acted as inhibitors of the EROD activities (having IC_{50} values below 10 μM). The azole omeprazole, on the other hand, did not significantly inhibit EROD activities (having an IC_{50} value above 50 μM), and there was no synergistic mixture effect when BNF was mixed with omeprazole.[21] This supports our hypothesis that inhibition of CYP1A activities triggers a synergistic mixture effect. A similar synergistic mixture effect on the CYP1A biomarker has been observed in cells exposed to another AhR agonist, the polycyclic aromatic hydrocarbon benzo[*a*]pyrene, in combination with an antifungal imidazole drug clotrimazole (Alvord, C.; Lundh, T.; Wiklander, K.; Bernhardsson, A.; Celander, M.C. data not shown). Hence, the model has a potential to be used for other chemical mixtures.

Sensitivity and identifiability analysis revealed that the parameter corresponding to the rate of CYP1A enzyme degradation is the most influential parameter on the dynamics of the EROD activity of free CYP1A enzymes predicted by the model. In contrast, the parameter related to biotransformation of BNF is the parameter with the least individual influence on this variable. Hence, to reduce the total uncertainty in the model predictions for the EROD activity of CYP1A enzymes, the parameter corresponding to the rate of CYP1A enzyme degradation should be estimated with low uncertainty. The present study provides a new promising toxicokinetic model with predictive power to describe synergistic mixture effects between aromatic hydrocarbons and azoles.

■ ASSOCIATED CONTENT

Supporting Information

The Supporting Information is available free of charge at https://pubs.acs.org/doi/10.1021/acs.est.0c04839.

Raw data for EROD activities in seven treatment groups from the previously published study;[21,22] raw data from a dose−response experiment with BNF alone on EROD activities at 24 h in vehicle control (DMSO)-treated cells and in cells treated with 0.1, 0.3, 0.9, 1, 3, 8, or 25 μM BNF alone from the previously published study;[22] raw data from dose response experiment with NOC alone on EROD activities at 6, 12, 24, 48, and 72 h in vehicle control (DMSO)-treated cells and in cells treated with 1, 10, or 25 μM NOC alone from the previously published study;[21,22] sensitivity values of the 10 parameters at each time point for the six treatments; and collinearity index for all parameter combinations (PDF)

■ AUTHOR INFORMATION

Corresponding Author

Malin C. Celander − *Department of Biological and Environmental Sciences, University of Gothenburg, Gothenburg SE 405 30, Sweden;* orcid.org/0000-0002-4350-751X; Phone: +46 (0)31 786 3693; Email: malin.celander@gu.se

Authors

Shirin Fallahi − *Department of Mathematics, University of Bergen, Bergen N 5020, Norway*

Marie Mlnaříková − *Department of Biological and Environmental Sciences, University of Gothenburg, Gothenburg SE 405 30, Sweden*

Charlotte Alvord − *Department of Biological and Environmental Sciences, University of Gothenburg, Gothenburg SE 405 30, Sweden*

Guttorm Alendal − *Department of Mathematics, University of Bergen, Bergen N 5020, Norway*

Håvard G. Frøysa − *Department of Mathematics, University of Bergen, Bergen N 5020, Norway*

Torbjörn Lundh − *Mathematical Sciences, Chalmers University of Technology and the University of Gothenburg, Gothenburg SE 412 96, Sweden;* orcid.org/0000-0001-7081-1384

Complete contact information is available at: https://pubs.acs.org/10.1021/acs.est.0c04839

https://dx.doi.org/10.1021/acs.est.0c04839
Environ. Sci. Technol. 2020, 54, 13748−13758

Author Contributions

T.L. created the initial model. S.F. performed the mathematical modeling and mathematical analysis and cowrote the manuscript. M.M. performed the time course experiments and the EROD analyses and commented on the manuscript. C.A. participated in the discussions and meetings, before leave of absence, and has approved the submission. G.A., H.F., and T.L. participated in the discussions and commented on the manuscript. M.C. supervised the study and cowrote the manuscript. S.F., M.M., H.F., G.A., T.L., and M.C. have participated in the revision process and have read and approved the final version of the manuscript.

Notes

The authors declare no competing financial interest.

■ ACKNOWLEDGMENTS

This work was a contribution to the FORMAS project number 942-2015-605 to M.C. and T.L. and the dCod 1.0 project funded by the Research Council of Norway through grant number 248840 to S.F., H.F., G.A., and M.C. We thank Libe Aranguren-Abadía from the Department of Biosciences at University of Bergen for helping with preparing the graphics.

■ ABBREVIATIONS

AhR	aryl hydrocarbon receptor
BNF	β-naphthoflavone
CYP1A	cytochrome P450 1A
GSA	global sensitivity analysis
EROD	ethoxyresorufin-*O*-deethylase
FME	flexible modeling environment
LSA	local sensitivity analysis
NOC	nocodazole
ODE	ordinary differential equation
PLHC-1	*Poeciliopsis lucida* hepatocellular carcinoma

■ REFERENCES

(1) Hinton, D. E.; Segner, H.; Au, D. W. T.; Kullman, S. W.; Hardman, R. C. Liver Toxicity. In *The Toxicology of Fishes*; Di Gulio, R. T., Hinton, D. E., Eds.; CRS Press. Taylor & Francis Group, 2008, Chapter 7; pp 328−352.

(2) Fent, K.; Weston, A.; Caminada, D. Ecotoxicology of human pharmaceuticals. *Aquat. Toxicol.* **2006**, *76*, 122−159.

(3) Corcoran, J.; Winter, M. J.; Tyler, C. R. Pharmaceuticals in the aquatic environment: A critical review of the evidence for health effects in fish. *Crit. Rev. Toxicol.* **2010**, *40*, 287−304.

(4) Celander, M. C. Cocktail effects on biomarker responses in fish. *Aquat. Toxicol.* **2011**, *105*, 72−77.

(5) Groten, J. P.; Feron, V. J.; Sühnel, J. Toxicology of simple and complex mixtures. *Trends Pharmacol. Sci.* **2001**, *22*, 316−322.

(6) Hadrup, N.; Taxvig, C.; Pedersen, M.; Nellemann, C.; Hass, U.; Vinggaard, A. M. Concentration addition, independent action and generalized concentration addition models for mixture effect prediction of sex hormone synthesis in vitro. *PLoS One* **2013**, *8*, No. e70490.

(7) Rajapakse, N.; Silva, E.; Scholze, M.; Kortenkamp, A. Deviation from additivity with estrogenic mixtures containing 4-nonylphenol and 4-tert-octylphenol detected in the E-SCREEN assay. *Environ. Sci. Technol.* **2004**, *38*, 6343−6352.

(8) Crofton, K. M.; Craft, E. S.; Hedge, J. M.; Gennings, C.; Simmons, J. E.; Carchman, R. A.; Carter, W. H., Jr.; DeVito, M. J. Thyroid-hormone−disrupting chemicals: evidence for dose-dependent additivity or synergism. *Environ. Health Perspect.* **2005**, *113*, 1549−1554.

(9) Hass, U.; Scholze, M.; Christiansen, S.; Dalgaard, M.; Vinggaard, A. M.; Axelstad, M.; Metzdorff, S. B.; Kortenkamp, A. Combined exposure to anti-androgens exacerbates disruption of sexual differentiation in the rat. *Environ. Health Perspect.* **2007**, *115*, 122−128.

(10) Charles, G. D.; Gennings, C.; Tornesi, B.; Kan, H. L.; Zacharewski, T. R.; Bhaskar Gollapudi, B.; Carney, E. W. Analysis of the interaction of phytoestrogens and synthetic chemicals: an in vitro/in vivo comparison. *Toxicol. Appl. Pharmacol.* **2007**, *218*, 280−288.

(11) Bobb, S.; Berggren, E.; Kienzler, A.; van der Linden, S.; Wort, A. *Scientific Methodologies for the Assessment of Combined Effects of Chemicals − A Survey and Literature Review. Use of Novel and Alternative Methods in the Assessment of Effects from Combined Exposure to Multiple Chemicals*, JRC Technical Reports. EUR 27471 EN, 2015.

(12) Cedergreen, N.; Dalhoff, K.; Li, D.; Gottardi, M.; Kretschmann, A. C. Can toxicokinetic modeling be used to understand and predict synergistic interactions between chemicals? *Environ. Sci. Technol.* **2017**, *51*, 14379−14389.

(13) Bach, J.; Snegaroff, J. Effects of the fungicide prochloraz on the xenobiotic metabolism in Rainbow trout − in vivo induction. *Xenobiotica* **1989**, *19*, 1−9.

(14) Levine, S. L.; Czosnyka, H.; Oris, J. T. Effects of the fungicide clotrimazole on bioconcentration of benzo[a]pyrene in gizzard shad (Dorosoma cepedianum): In vivo and in vitro inhibition of CYP1A activity. *Environ. Toxicol. Chem.* **1997**, *16*, 306−311.

(15) Egaas, E.; Sandvik, M.; Fjeld, E.; Källqvist, T.; Goksøyr, A.; Svensen, A. Some effects of the fungicide propiconazole on cytochrome P450 and glutathione S-transferase in brown trout (Salmo trutta). *Comp. Biochem. Physiol., Part C: Pharmacol., Toxicol. Endocrinol.* **1999**, *122*, 337−344.

(16) Sturm, A.; Cravedi, J. P.; Perdu, E.; Baradat, M.; Segner, H. Effects of prochloraz and nonylphenol diethoxylate on hepatic biotransformation in trout: A comparative in vitro/in vivo-assessment using cultured hepatocytes. *Aquat. Toxicol.* **2001**, *53*, 229−245.

(17) Hegelund, T.; Ottosson, K.; Rådinger, M.; Tomberg, P.; Celander, M. C. Effects of ketoconazole on CYP1A and CYP3A in rainbow trout and killifish. *Environ. Toxicol. Chem.* **2004**, *23*, 1326−1334.

(18) Hasselberg, L.; Grøsvik, B. E.; Goksøyr, A.; Celander, M. C. Interactions between xenoestrogens and ketoconazole on CYP1A and CYP3A in juvenile Atlantic cod (Gadus morhua). *Comp. Hepatol.* **2005**, *4*, 2.

(19) Hasselberg, L.; Westerberg, S.; Wassmur, B.; Celander, M. C. Ketoconazole, an antifungal imidazole, increases the sensitivity of rainbow trout to 17α-ethynylestradiol exposure. *Aquat. Toxicol.* **2008**, *86*, 256−264.

(20) Wassmur, B.; Gräns, J.; Norström, E.; Wallin, M.; Celander, M. C. Interactions of pharmaceuticals and other xenobiotics on key detoxification mechanisms and cytoskeleton in Poeciliopsis lucida hepatocellular carcinoma, PLHC-1 cell line. *Toxicol. In Vitro* **2013**, *27*, 111−120.

(21) Gräns, J.; Johansson, J.; Michelová, M.; Wassmur, B.; Norström, E.; Wallin, M.; Celander, M. C. Mixture effects between different azoles and β-naphthoflavone on the CYP1A biomarker in a fish cell line. *Aquat. Toxicol.* **2015**, *164*, 43−51.

(22) Michelová, M. Cocktail Effects of β-naphthoflavone and Nocodazole in the Poeciliopsis lucida Cell Line. Master-thesis, University of Gothenburg, 2012.

(23) Segner, H. Fish cell lines as a tool in aquatic toxicology. In *Fish Ecotoxicology*; Branbeck, T., Hinton, D. E., Streit, B., Eds.; Springer Basel AG, 1998; Vol. *86*; pp 1−38.

(24) Fent, K. Fish cell lines as versatile tools in ecotoxicology: assessment of cytotoxicity, cytochrome P4501A induction potential and estrogenic activity of chemicals and environmental samples. *Toxicol. In Vitro* **2001**, *15*, 477−488.

(25) Celander, M.; Bremer, J.; Hahn, M. E.; Stegeman, J. J. Glucocorticoid-xenobiotic interactions: dexamethasone-mediated potentiation of cytochrome P4501A by ß-naphthoflavone in a fish hepatoma cell line (PLHC-1). *Environ. Toxicol. Chem.* **1997**, *16*, 900−907.

https://dx.doi.org/10.1021/acs.est.0c04839
Environ. Sci. Technol. 2020, 54, 13748−13758

(26) R Core Team. R A language and environment for statistical computing; R Foundation for Statistical Computing: Vienna, Austria, 2020, URL https://www.R-project.org/.
(27) Tofallis, C. A better measure of relative prediction accuracy for model selection and model estimation. *J. Oper. Res. Soc.* **2015**, *66*, 1352−1362.
(28) Soetaert, K.; Petzoldt, T. Inverse modelling, sensitivity and monte carlo analysis in R using package FME. *J. Stat. Software* **2010**, *33*, 1−28.
(29) Soetaert, K.; Herman, P. M. *A Practical Guide to Ecological Modelling: Using R as a Simulation Platform*; Springer Science & Business Media, 2008.
(30) Soetaert, K. E.; Petzoldt, T.; Setzer, R. W. Solving differential equations in R: package deSolve. *J. Stat. Software* **2010**, *33*, 6−7.
(31) Gábor, A.; Villaverde, A. F.; Banga, J. R. Parameter identifiability analysis and visualization in large-scale kinetic models of biosystems. *BMC Syst. Biol.* **2017**, *11*, 1−16.
(32) Brun, R.; Reichert, P.; Künsch, H. R. Practical identifiability analysis of large environmental simulation models. *Water Resour. Res.* **2001**, *37*, 1015−1030.
(33) Pilling, E. D.; Bromleychallenor, K. A. C.; Walker, C. H.; Jepson, P. C. Mechanism of synergism between th pyrethroid insecticide lambda-cyhalothrin and the imidazole fungicide prochloraz, in the honeybee (Apis mellifera L.). *Pestic. Biochem. Physiol.* **1995**, *51*, 1−11.
(34) Gottardi, M.; Cedergreen, N. The synergistic potential of azole fungicides does not directly correlate to the inhibition of cytochrome P450 activity in aquatic invertebrates. *Aquat. Toxicol.* **2019**, *207*, 187−196.
(35) Gottardi, M.; Tyzack, J. D.; Bender, A.; Cedergreen, N. Can the inhibition of cytochrome P450 in aquatic invertebrates due to azole fungicides be estimated with in silico and in vitro models and extrapolated between species? *Aquat. Toxicol.* **2018**, *201*, 11−20.
(36) Stadnicka-Michalak, J.; Weiss, F. T.; Fischer, M.; Tanneberger, K.; Schirmer, K. Biotransformation of benzo[a]pyrene by three rainbow trout (Onchorhynchus mykiss) cell lines and extrapolation to derive fish bioconcentration factor. *Environ. Sci. Technol.* **2018**, *52*, 3091−3100.

https://dx.doi.org/10.1021/acs.est.0c04839
Environ. Sci. Technol. 2020, 54, 13748−13758